Slab deformation in the mid–mantle

Marie Behounkova & Hana Cizkova

e-mail: Marie.Behounkova@mff.cuni.cz WWW: http://geo.mff.cuni.cz/~behounek

Charles University in Prague, Faculty of Mathematics and Physics, Department of Geophysics, Prague, Czech Republic

Introduction

Results of high resolution seismic tomography show significant thickening of the slabs in the lower mantle. Ribe et al. 2007 suggest that the width of the subducting plate can be up to more then $400\,\mathrm{km}$ in the regions of Central America and Java. In regions such as Mariana, Kuril-Kamchatka and Tonga, the plate is thickened by factors up to five. This slabs thickening in the lower mantle can have important consequences in global geodynamics (e.g. geoid interpretation). To be able to explain the long-wavelength character in the lower mantle, two possible mechanisms are usually considered: either the compression of the plate material due to the high resistance of the lower mantle or the buckling of the plate.

We employ forward modelling method based on Gerya and Yuen (2003) to study the circumstances under which the thickening of the subducting plates occurs. We consider thermo-chemical model with two materials - mantle material (0) and decoupling layer material (1). The major phase transitions at the depths $400\,\mathrm{km}$ and $670\,\mathrm{km}$ and composite rheology including diffusion creep, dislocation creep and stress limiting mechanism are taken into account. We prescribe either horizontal velocity of free-slip condition on the top boundary. We study the influence of viscosity jump in the lower mantle $C = 1,\ 10$ and 30, viscosity of decoupling layer η_{DL} varying between $10^{19}\,\mathrm{Pa}\cdot\mathrm{s}$ and $5\cdot10^{21}\,\mathrm{Pa}\cdot\mathrm{s}$ and we test yield stress σ_{y} between $5\cdot10^{7}\,\mathrm{Pa}$ and $10^{9}\,\mathrm{Pa}$.

Method and Model Setup

- finite difference code in 2-D Cartesian box based on Gerya & Yuen (2003), incompressible fluid in extended Boussinesq approximation
- governing equations in the dimensionless form:

$$\nabla\cdot\boldsymbol{v} = 0$$

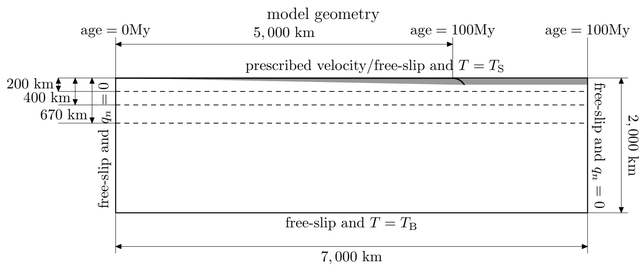
$$-\nabla\pi + \nabla\cdot\boldsymbol{\sigma} = \left(Ra\frac{\alpha}{\alpha_S}(T-T_0) - \sum_k Rb_k\Gamma_k\right)\frac{\boldsymbol{g}}{g_0}$$

$$\frac{\partial T}{\partial t} = \nabla\cdot k\nabla T - \boldsymbol{v}\cdot\nabla T + Di\frac{\alpha}{\alpha_S}\left(T+\frac{T_S}{T_B-T_S}\right)\frac{\boldsymbol{g}}{g_0}\cdot\boldsymbol{v} + \frac{D_S}{Ra_S}\boldsymbol{\sigma}:\nabla\boldsymbol{v} + \sum_k\frac{Rb_k}{Ra}Di\left(T+\frac{T_S}{T_B-T_S}\right)\gamma_k\frac{\mathrm{D}\Gamma_k}{\mathrm{D}t}$$

- chemical composition: mantle material (0) and decoupling layer material (1) with no density anomaly
- mantle material rheology: combining diffusion creep, dislocation creep and general stress limiting creep mechanism

diffusion creep	$\eta_{\mathrm{diff}} = C\,A_{\mathrm{diff}}^{-1}\exp\left(\frac{E^*_{\mathrm{diff}}+PV_{\mathrm{diff}}}{RT}\right)$
dislocation creep	$\eta_{\mathrm{disl}} = C\,A_{\mathrm{disl}}^{-1/n}\dot{e}^{(1-n)/n}\exp\left(\frac{E^*_{\mathrm{disl}}+PV_{\mathrm{disl}}}{RT}\right)$
stress limiting viscosity	$\eta_{\mathrm{y}} = C\,\sigma_y\dot{e}_y^{-1/n_y}\dot{e}^{1/n_y-1}$
effective viscosity (van den Berg et al., 1993)	$\eta = \left(\frac{1}{\eta_{\mathrm{diff}}}+\frac{1}{\eta_{\mathrm{disl}}}+\frac{1}{\eta_y}+\frac{1}{\eta_{\max}}\right)^{-1}$

- decoupling layer viscosity is constant up to $200\,\mathrm{km}$ and it has the same rheological properties as mantle material for greater depths, the thickness of the decoupling layer is $10\,\mathrm{km}$ and constitutes top part of the subducting plate



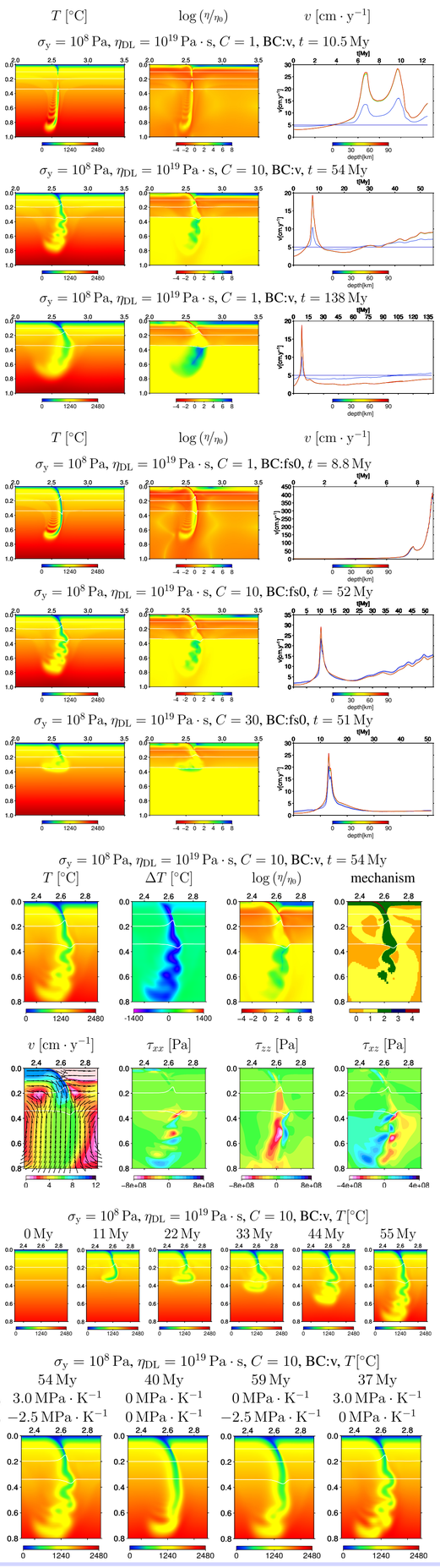
gravity acceleration	g_0	$10\ \mathrm{m\cdot s^{-2}}$
height	d	$2,000\ \mathrm{km}$
surface temperature	T_{S}	$273\ \mathrm{K}$
bottom temperature	T_{B}	$2,753\ \mathrm{K}$
density	ρ_0	$3,400\ \mathrm{kg\cdot m^{-3}}$
thermal conductivity	k	$5\ \mathrm{W\cdot m^{-1}\cdot K^{-1}}$
heat capacity	c_{p}	$1,250\ \mathrm{J\cdot kg^{-1}\cdot K^{-1}}$
thermal expansion coefficient	α	$3.5\cdot10^{-6}\ \mathrm{K^{-1}}$
plate velocity	$v_{x\ \mathrm{BC}}$	$5\ \mathrm{cm\cdot y^{-1}}$
molar gas constant	R	$8.3143\ \mathrm{J\cdot K^{-1}\cdot mol^{-1}}$
maximal viscosity	$\eta_{\max}$	$10^{28}\ \mathrm{Pa\cdot s}$
reference viscosity	η_0	$10^{21}\ \mathrm{Pa\cdot s}$
upper mantle parameters (material 0):[1]		
pre-exponential parameter of diffusion creep	A_{diff}	$1.92\cdot10^{-10}\ \mathrm{Pa^{-1}\cdot s^{-1}}$
activation energy for diffusion creep	E^*_{diff}	$300\cdot10^{3}\ \mathrm{J\cdot mol^{-1}}$
activation volume for diffusion creep	V^*_{diff}	$6.0\cdot10^{-6}\ \mathrm{m^3\cdot mol^{-1}}$
pre-exponential parameter of dislocation creep	A_{disl}	$2.42\cdot10^{-16}\ \mathrm{Pa^{-n}\cdot s^{-1}}$
activation energy for dislocation creep	E^*_{disl}	$540\cdot10^{3}\ \mathrm{J\cdot mol^{-1}}$
activation volume for dislocation creep	V^*_{disl}	$15\cdot10^{-6}\ \mathrm{m^3\cdot mol^{-1}}$
viscosity stress exponent	n	3.5
lower mantle parameters (material 0):[2]		
pre-exponential parameter of diffusion creep	A_{diff}	$3.65\cdot10^{-15}\ \mathrm{Pa^{-1}\cdot s^{-1}}$
activation energy for diffusion creep	E^*_{diff}	$208\cdot10^{3}\ \mathrm{J\cdot mol^{-1}}$
activation volume for diffusion creep	V^*_{diff}	$2.5\cdot10^{-6}\ \mathrm{m^3\cdot mol^{-1}}$
pre-exponential parameter of dislocation creep	A_{disl}	$6.63\cdot10^{-32}\ \mathrm{Pa^{-n}\cdot s^{-1}}$
activation energy for dislocation creep	E^*_{disl}	$285\cdot10^{3}\ \mathrm{J\cdot mol^{-1}}$
activation volume for dislocation creep	V^*_{disl}	$1.37\cdot10^{-6}\ \mathrm{m^3\cdot mol^{-1}}$
viscosity stress exponent	n	3.5
yield stress	σ_y	$10^{8}, 10^{9}\ \mathrm{Pa}$
reference strain rate in yield strength determination	$\dot{\varepsilon}_y$	$10^{-15}\ \mathrm{s^{-1}}$
yield stress exponent	n_y	5
viscosity of decoupling layer (material 1)	η_{DL}	$10^{19},\ 10^{21}\ \mathrm{Pa\cdot s}$
coefficient of the viscosity jump at $670\,\mathrm{km}$ boundary	C	1, 10, 30
Clapeyron slope 400 km phase transition[3]	γ_{400}	$3.0\ \mathrm{MPa\cdot K^{-1}}$
density difference across 400 km phase transition[4]	$\Delta\rho_{400}$	$273\ \mathrm{kg\cdot m^{-3}}$
Clapeyron slope 670 km phase transition[3]	γ_{670}	$-2.5\ \mathrm{MPa\cdot K^{-1}}$
density difference across 670 km phase transition[4]	$\Delta\rho_{670}$	$342\ \mathrm{kg\cdot m^{-3}}$
width of all phase transitions	d_{ph}	$5\ \mathrm{km}$

[1] Karato and Wu 1993
[2] Yamazaki and Karato (2001), Frosth and Ashby (1982)
[3] Bina and Helffrich (1994)
[4] Steinbach and Yuen (1995)

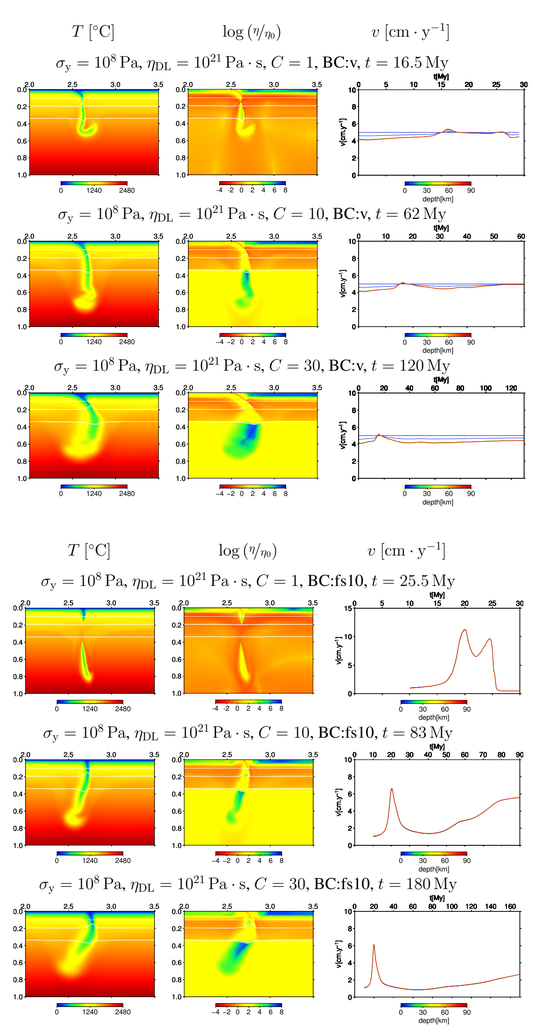
Conclusions

- We present the results of parametric study (Běhounková and Čížková, 2008), which aims at finding rheological parameters producing the slabs thickening in the lower mantle.
- Models with lower yield stress $\sigma_{\mathrm{y}} = 10^{8}\,\mathrm{Pa}$
  - For most of the models with no viscosity jump, the plates break at $\sim 400\,\mathrm{km}$ after their tip penetrates into the lower mantle. The only exception is the model with free-slip and weak decoupling layer, where the slab penetrates into the lower mantle without detachment and significant deformation.
  - For models with viscosity jump $C = 10$, the shape of the slab depends on the strength of the decoupling layer. For the weaker decoupling layer, the buckling occurs in the lower mantle and the estimated plate width is $\sim 400\,\mathrm{km}$. For the stronger decoupling layer, the plate deflects at $670\,\mathrm{km}$ boundary and then penetrates into the lower mantle without significant thickening.
  - For models with viscosity jump $C = 30$, the buckling instabilities occur for models with prescribed velocity. The maximum slabs widths are $450\,\mathrm{km}$ and $650\,\mathrm{km}$ for models with weaker and stronger decoupling layer, respectively. For model with stronger decoupling layer and free-slip condition, the plate penetrates slowly into the lower mantle and the plate thickening is observed due to compression and heat conduction. The slab width is approximately $350\,\mathrm{km}$.
- Models with higher yield stress $\sigma_{\mathrm{y}} = 10^{9}\,\mathrm{Pa}$
  - For models with no viscosity jump and viscosity jump $C = 10$, the plates penetrate into the lower mantle without significant thickening. The shapes of the subducting plates depend on prescribed boundary condition, viscosity jump and strength of the decoupling layer.
  - For models with viscosity jump $C = 30$, the subducting process is almost stopped at $670\,\mathrm{km}$ boundary. Only for model with sufficient push (prescribed velocity on the top boundary and stronger decoupling layer), the slab strongly deforms but finally penetrates into the lower mantle.
- In models with no viscosity jump, unrealistically high plate velocities are observed. This effect can be caused by rather low viscosity of the lower mantle, by underestimation of the friction on the plates contact or it can be an effect of 2-D geometry.
- The presence of the major phase transitions support formation of the buckling instabilities.

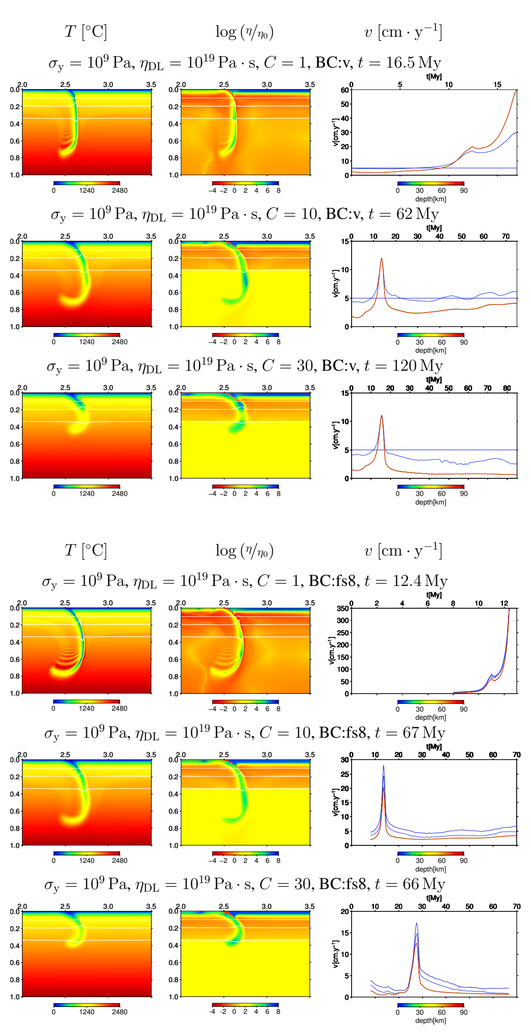
$\sigma_y = 10^8$ Pa $\eta_{DL} = 10^{19}$ Pa s



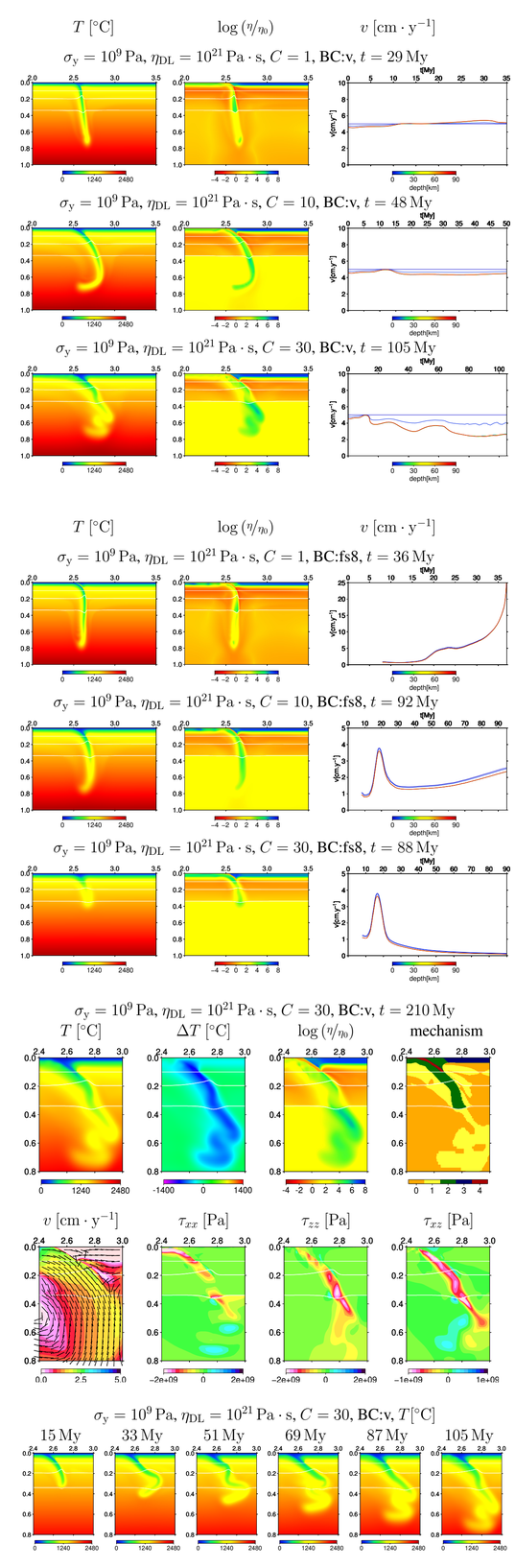
$\sigma_y = 10^8$ Pa $\eta_{DL} = 10^{21}$ Pa s



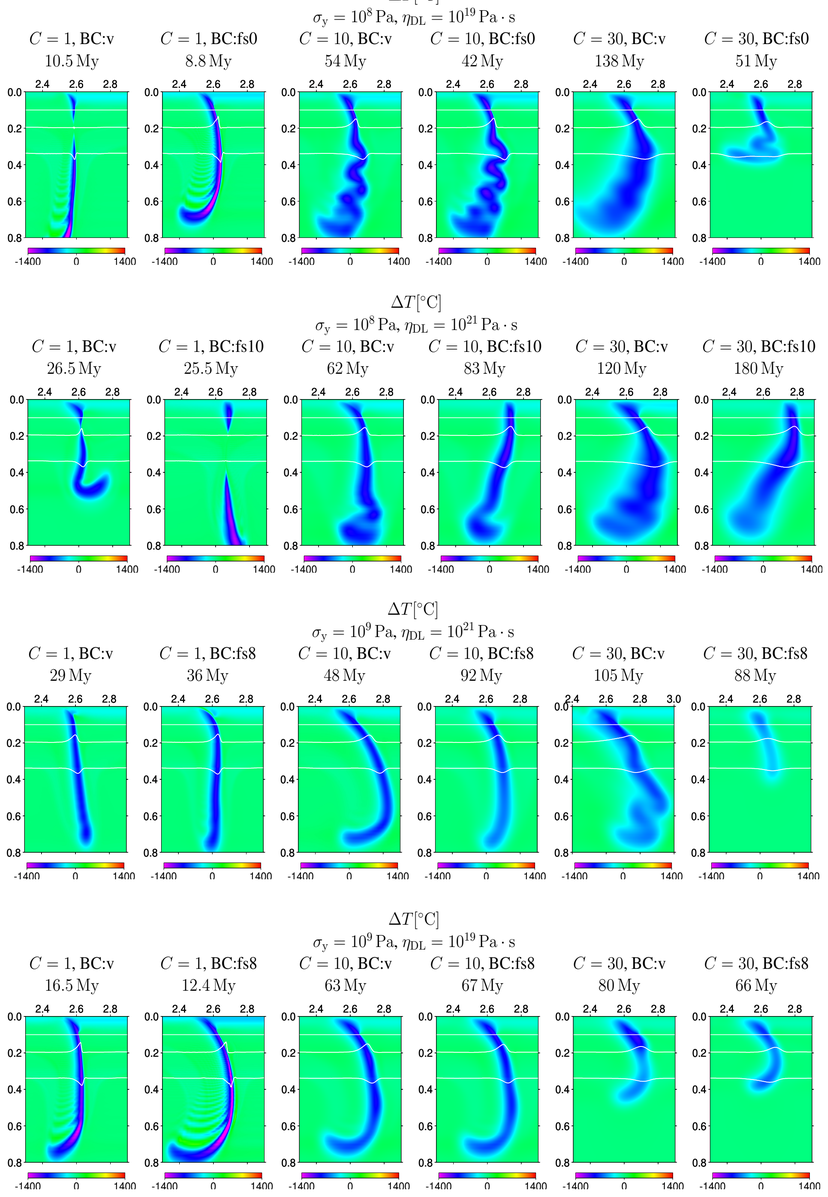
$\sigma_y = 10^9$ Pa $\eta_{DL} = 10^{19}$ Pa s



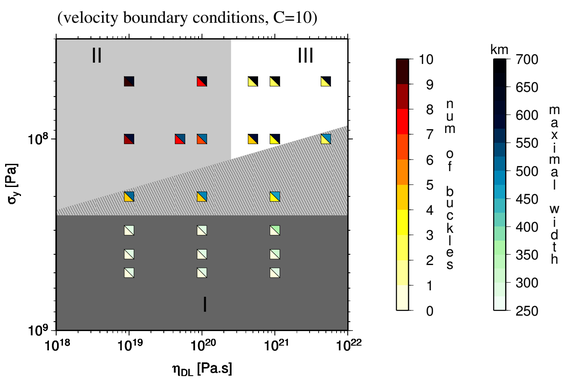
$\sigma_y = 10^9$ Pa $\eta_{DL} = 10^{21}$ Pa s



Summary



Phase Diagram



References

M. Běhounková & H. Čížková (2008). Long-wavelength character of subducted slabs in the lower mantle, Earth Planet. Sci. Lett. 275, 43-53.

C. Bina & G. Hellfrich (1994). Phase transition Clapeyron slopes and transition zone seismic discontinuity topography, J. Geophys. Res. 103, 15853-15860.

H.J. Frost & M.F. Ashby (1982). Deformation mechanism maps, Pergamon Press Oxford.

T.V. Gerya & D.A. Yuen (2003). Characteristics-based marker-in-cell method with conservative finite-differences schemes for modeling geological flows with strongly variable transport properties, Phys. Earth Planet. Inter. 140, 293-318.

S.-I. Karato & P. Wu (1993). Rheology of the upper mantle: a synthesis, Science 260, 83-108.

N.M. Ribe, E. Stutzmann, Y. Ren & R. van der Hilst (2007). Buckling instabilities of subducted lithosphere beneath the transition zone, Earth Plan. Sci. Let. 254, 173-179.

V. Steinbach & D.A. Yuen (1995). The effects of temperature dependent viscosity on mantle convection with two mantle major phase transitions, Phys. Earth Plan. Inter. 90, 13-36.

A. van den Berg, P. van Keken & D.A. Yuen (1993). The effects of a composite non-newtonian and newtonian rheology on mantle convection, Geophys. J. Int. 115, 62-78.

D. Yamazaki & S.-I. Karato (2001). Some mineral physics constraints on the rheology and geothermal structure of Earth's lower mantle, American Mineralogist, 86, 385-391.